Regularization Based Iterative Point Match Weighting for Accurate Rigid Transformation Estimation

Yonghuai Liu, *Senior Member, IEEE* Luigi De Dominicis, Baogang Wei, Liang Chen, Ralph R. Martin

Abstract—Feature extraction and matching (FEM) for 3D shapes finds numerous applications in computer graphics and vision for object modeling, retrieval, morphing, and recognition. However, unavoidable incorrect matches lead to inaccurate estimation of the transformation relating different datasets. Inspired by AdaBoost, this paper proposes a novel iterative re-weighting method to tackle the challenging problem of evaluating point matches established by typical FEM methods. Weights are used to indicate the degree of belief that each point match is correct. Our method has three key steps: (i) estimation of the underlying transformation using weighted least squares, (ii) penalty parameter estimation via minimization of the weighted variance of the matching errors, and (iii) weight re-estimation taking into account both matching errors and information learnt in previous iterations. A comparative study, based on real shapes captured by two laser scanners, shows that the proposed method outperforms four other state-of-the-art methods in terms of evaluating point matches between overlapping shapes established by two typical FEM methods, resulting in more accurate estimates of the underlying transformation. This improved transformation can be used to better initialize the iterative closest point algorithm and its variants, making 3D shape registration more likely to succeed.

Index Terms—Feature extraction; Feature matching; Point match evaluation; Iterative re-weighting; Rigid transformation; Registration

1 Introduction

Object modeling, recognition, morphing, and retrieval are widely used tasks in computer graphics and vision. A common basis for performing such tasks relies on using feature extraction and matching (FEM) methods to analyse overlapping range images captured from different viewpoints, each representing part of an object's surface shape (see Figure 1).

The features extracted typically depend on surface structure around each point, matching proceeding by identifying points in other range images with similar neighbourhoods. Identified points may then be used to register the partial shapes, a key output being to estimate the underlying transformation that best aligns them. Having found the transformation, if point correspondences between the partial shapes are needed, they can be easily identified as point pairs with small enough distances. In this paper, we consider the underlying transformation to be a rigid motion involving a rotation and translation, but our method is in principle also applicable to more general classes of transformation such as thin plate spline (TPS) deformations [21].

Feature extraction and matching are widely used to register overlapping partial shapes [15], [19], [32], [33]. This approach is applicable to shapes with varying complexities of geometry, varying degrees of overlap, and varying magnitudes of transformation. The signature of histograms of orientations (SHOT) [32] method is one of the best methods for the extraction and matching of features from overlapping partial shapes [4]. Even so, it usually unavoidably includes outliers amongst the point matches established, and typically a random sample consensus (RANSAC) scheme [9] is used to reject them. The unit quaternion method [5] is then used to estimate the underlying transformation. However, the RANSAC scheme has a number of shortcomings [29], including, computational inefficiency, and the need to select thresholds determining whether a match is an inlier or outlier, and when a good model has been found. In this paper, we propose a novel, alternative, iterative re-weighting method for evaluating the point matches established, with the aim of estimating the underlying transformation as accurately as possible. This estimate might typically be used to initialize a variant [17], [30] of the iterative closest point (ICP) algorithm [5] for final refinement of the transformation. A particular concern is whether our approach provides an estimated transformation closer to the globally optimal solution than

- *Y. Liu is with the Department of Computer Science, Aberystwyth University, Ceredigion SY23 3DB, UK. Email:yyl@aber.ac.uk*
- *L.D. Dominics is with the Diagnostics and Metrology Laboratory UTAPRAD-DIM, 00044 ENEA Frascati, Italy. Email: luigi.dedominicis@enea.it*
- *B. Wei is with the College of Computer Science and Technology, Zhejiang University, Hangzhou, 310027, P.R. China. Email: wbg@zju.edu.cn*
- *L. Chen is with the Computer Science Department, University of Northern British Columbia, 3333 University Way, Prince George, BC V2N 4Z9, Canada. Email: liang.chen@unbc.ca*
- *R.R. Martin is with the School of Computer Science & Informatics, Cardiff University, Cardiff CF24 3AA, UK. Email: ralph@cs.cf.ac.uk*

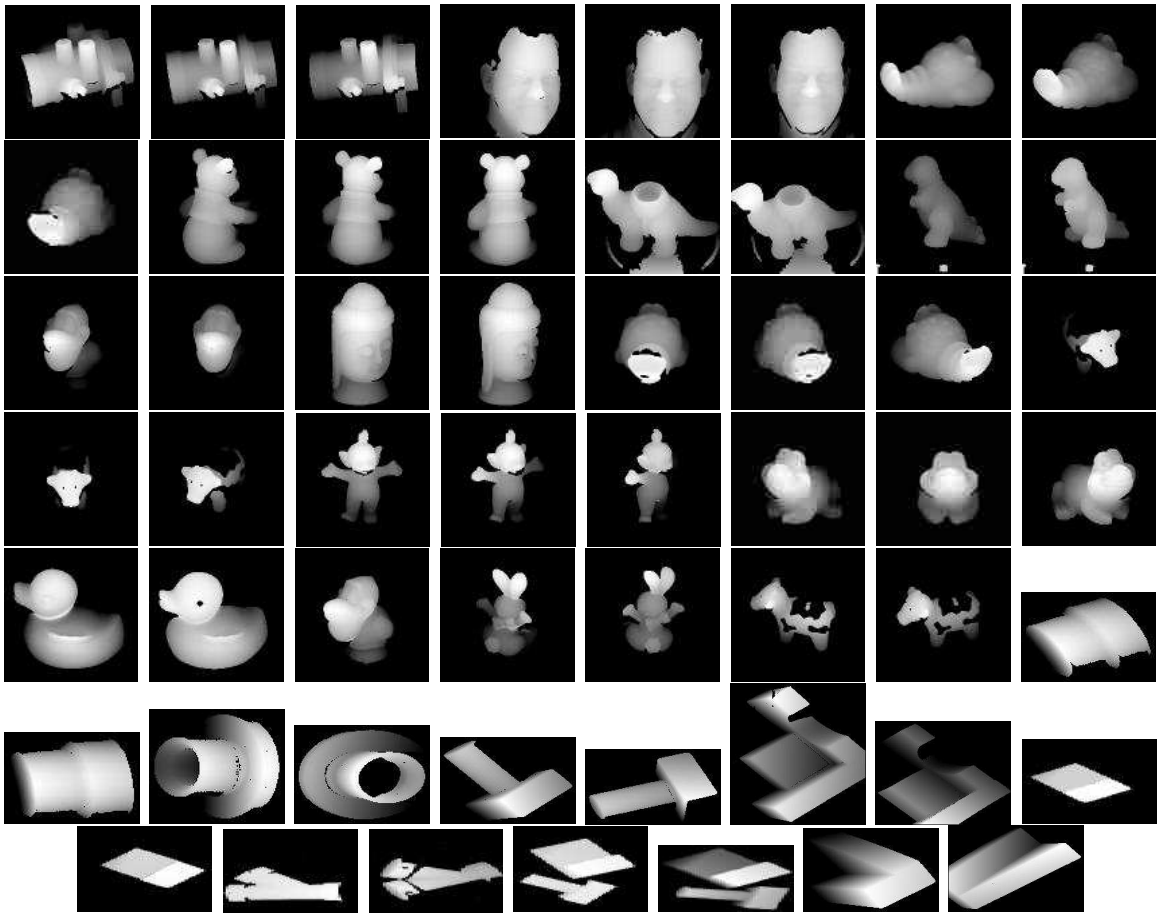

Fig. 1. Real range images used in testing. From left to right: Row 1: valve20, valve10, valve0, pat108, pat144, pat180, lobster0 and lobster20. Row 2: lobster40, pooh140, pooh160, pooh180, bluedino125, bluedino375, reddino0 and reddino36. Row 3: bird20, bird40, buddha40, buddha60, lobster60, lobster80, lobster100 and cow50. Row 4: cow47, cow44, tubby0, tubby20, tubby40, frog0, frog40 and frog80. Row 5: duck0, duck20, bird0, bunny0, bunny40, cow37, cow40 and adapter2. Row 6: adapter3, agpart2, agpart3, column2, column5, curvblock1, curvblock2 and grn-blk1. Row 7: grn-blk2, wye2, wye3, jumble11, jumble12, block2, and block3.

the one provided by the original SHOT method—if it does, it is more likely [37] that the ICP variant will converge correctly to the global optimum, rather than a local optimum.

The adaptive boosting (AdaBoost) method [10] is a powerful, well-known machine learning tool for data classification. It iteratively increases the weights of incorrectly classified data and decreases the weights of correctly classified data. Based on such weights, different weak classifiers can be trained. The output of several weak learners is combined into a weighted sum that represents the final output of the boosted classifier. AdaBoost is adaptive in the sense that subsequent weak learners are tweaked in favor of those instances misclassified by previous classifiers. AdaBoost is sensitive to noisy data and outliers, but in some problems it can be less susceptible to overfitting than other learning algorithms. The individual learners can be weak, but as long as the performance of each one is at least somewhat better than random guessing (i.e. has an error rate less than 0.5), the final model can be proven to converge to a strong learner [1]. A careful analysis shows that AdaBoost actually possesses three useful properties: (i) it allows a direct selection of the best solution across different iterations; (ii) the final solution can be estimated as a weighted average of outputs provided by different weak classifiers; and (iii) it provides as a byproduct an estimate of the reliability with which each data item is a good fit to the final model.

Inspired by the above third property of AdaBoost, we propose a novel iterative re-weighting method for evaluating point matches established through FEM [15], [19], [32], [33]. Our main idea is as follows. Evaluation of the established point matches is essentially a data fitting problem: the putative point matches (PPMs) fit the underlying transformation. In our problem, all the established point matches belong to the same class and thus, unlike Adaboost, we do not have to deal with classification. Instead, we treat all the point matches in the same way for the fitting of the underlying transformation,

but as having different reliabilities or goodnesses. The reliability or weight of each point match is represented by a real number in the interval $[0, 1]$; the larger the number, the more likely we believe it to be correct, and the better it fits the underlying transformation. Lacking other knowledge, we initialize these weights equally. Once we have the PPMs and their weights, the underlying transformation can be estimated in a weighted least squares sense using the quaternion method [5]. This allows us to estimate the fitting errors of all the PPMs and thus their weighted mean e_μ and variance e_σ^2. We then focus on estimating and updating the reliability values iteratively. To do so, we construct an objective function that minimizes the weighted average of the matching errors with the weights regularized by their entropy. To balance the contribution of the two terms, instead of using a single parameter [13], we introduce a penalty parameter for each point match to characterize its unpredictable correctness. To estimate the penalty parameter, we construct another objective function that minimizes the variance from e_μ of the errors of the point matches weighted by twice the squares of these penalty parameters regularized by their shifted entropy. The two terms are balanced by $2e_\sigma^2$.

To make full use of and fuse the weights from different iterations, we maximize such weights over all previous iterations when estimating the reliability of each point match. The proposed method is based on regularization for iterative re-weighting and is thus refered to as RIRW in the rest of this paper. The above process is repeated until either a maximum number of iterations has been reached, or the weighted average fitting error is smaller than the average distance between the closest neighboring points in the original shapes.

We have validated our proposed RIRW method using real range scans from two publicly accessible databases [25] and also compare it to four state-of-the-art point match evaluation methods. The performance of each method is assessed using the relative differences between the rotation axis, rotation angle, and translation vector of the transformation estimated from the evaluated point matches, and those refined by a state-of-the-art ICP variant, SoftICP [17]. The experimental results show that the proposed RIRW method outperforms these competitors when evaluating point matches established by two representative FEM methods: the SHOT method [32] and the universal shape context (USC) method [33]. In all cases it yields smaller errors in the rotation axis, rotation angle, and translation vector. Furthermore, the estimated underlying transformation derived from the weighted point matches is closer to the global optimal solution, allowing the SoftICP algorithm to succeed in refinement.

The rest of this paper is structured as follows: Section 2 reviews related work, while Section 3 describes our proposed RIRW method. Section 4 presents an experimental evaluation using real data, and finally, Section 5 draws conclusions and indicates future work.

2 Related work

In this section, we review significant work on evaluation of point matches (established mainly by FEM methods), and uses of the AdaBoost classification method in computer vision.

2.1 Point match evaluation

Suggested point matches can take into account single points from each surface [15], pairs of points [7], or more (in higher-order point matching) [6], which successively improves the probability of finding correct matches. While higher-order point matching can usefully reduce outliers, it is computationally expensive due to the increased number of possibilities which must be considered. Indeed, to arrive at a computationally feasible method, such approaches are reduced to *sampling* potential matches, potentially discarding useful data. Whichever method is adopted, incorrect matches are unavoidably introduced, as real world data have areas of relatively featureless simple geometry, and because of imaging noise, holes, occlusion, appearance and disappearance of points, and cluttered backgrounds. All of these mean that the extracted features are typically not informative enough to enable points to be matched without ambiguity. The point matches established are typically heavily corrupted by outliers with gross errors, which in turn leads to inaccurate estimation of the underlying transformation. To overcome this problem, a means is needed to evaluate the quality or reliability of each match. Point match evaluation attempts to either classify the PPMs as inliers or outliers, or to characterize the extent to which each match is likely to be correct. In this paper, we adopt the second strategy to tackle the point match evaluation problem.

Li and Hu [16] were probably the first to consider evaluating established point matches, and various other work has followed. Methods used are based on one of three ideas (or a combination thereof): (i) *structural consistency* based methods verify whether the point matches adhere to structural constraints such as invariance of inter-point distances; (ii) *transformation consistency* based methods assume that all correct point matches share the same underlying transformation and thus have similar residuals after applying the correctly estimated transformation; and (iii) *statistical regression* methods use statistically robust functions to limit the influence of outliers when estimating the parameters of interest.

Structural consistency based methods assume that the correct point matches must have similar features and thus regard such point matches as false if their features are insufficiently similar. PPMs are filtered out in [15] using a feature similarity measure and geometric consistency. A point match that has low similarity of spin images and large geometric consistency distance between the coordinates of these spin images is regarded as an outlier. A match is deemed unreliable in [19] if the ratio between the dissimilarity of the best match and that

of the second best match is above a threshold. Possible correspondences between planes are refined in [27] using a set of consistency tests based on size, orientation, and position. Feature similarity scores and geometric consistency scores (using interpoint Euclidean distance) are used in [18] to define a weighted adjacency matrix when searching for common visual patterns between two images or shapes. Local isometry is considered in [31] (for non-rigid matching), using a diffusion method based on interpoint geodesic distances to prune false matches.

While feature similarity has already been employed for the identification of PPMs, structural consistency based methods may have difficulty in identifying other invariant features as a basis for the removal of false matches. Instead, *transformation consistency* based methods attempt first to estimate a consensus transformation and then consider the fitting errors of these matches under this transformation—a large fitting error usually implies that the corresponding match is an outlier. RANSAC [28], [32] is the basis for the most widely used transformation consistency based methods, typically operating on the residuals of point matches after transformation. A candidate underlying transformation is estimated from a sample of the PPMs, then all matches whose errors are smaller than a threshold are regarded as inliers, and finally all inliers are used to estimate the optimal transformation. A Hough transform (HT) approach is used in [19] to eliminate matching outliers. It is assumed in [16] that there is a linear correspondence function relating two images, which is estimated through support vector machine regression from the projections of the PPMs. Any match that does not satisfy the correspondence function is regarded as an outlier. Recently, Zhao et al have published a series of papers [39], [20], [21], [22], [23] on mismatch removal based on the assumption that the point matches undergo a coherent transformation which can be iteratively estimated by the expectation maximisation (EM) algorithm. While the underlying transformation between the PPMs is represented using TPS in [23] and a displacement field in [21], it is represented as a linear transformation in a reproducing kernel Hilbert space (RKHS) in [20], [22], [39].

The main goal for shape registration is to use the PPMs to estimate the underlying transformation that brings the two shapes into the best possible alignment, but robust statistical methods for regression allow this to be done in such a way that the reliable point matches make more contribution while others make little contribution. Typical methods are based on M-estimators [2], [16], [38], least median of squares, or RANSAC [9]. M-estimators require the definition of an influence function, and requires estimation of some tuning constants like the standard deviation of the data. The least median of squares method involves optimising a discontinuous objective function and is thus usually time consuming. RANSAC requires [29] choice of a threshold determining whether a point match is an inlier or outlier, and specifying how good a model is. Such thresholds are usually problem specific.

In contrast with existing methods which classify PPMs as inliers or outliers, we avoid making a hard decision by using real numbers in the unit interval to express our confidence in the extent to which they are correct.

After the initial transformation parameters have been estimated by FEM, they are typically refined using the (iterative) ICP algorithm [5] or one of its variants [17], [30]. The closer the initial underlying transformation is to the global minimum, the more likely the refinement will succeed. On the contrary, if the initial transformation estimate is not good enough, the refinement can fail catastrophically [37].

2.2 Boosting

The AdaBoost method [10] has received much attention from the machine learning community. It employs a set of weak learners to obtain strong solutions to data classification and learning problems, assuming that each weak classifier performs better than random guessing. It attempts to minimise the weighted sum of the exponential losses of the sample data. The main idea when training learners is to decrease the weights for correctly classified data instances and increase the weights for mis-classified instances, forcing the learning method to focus on the mis-classified instances. The iterative learning process has four main steps: given labelled instances are sampled, multiple weak classifiers are fitted and the one with a minimum weighted average of errors is identified, the boosting parameter is estimated as a function of the minimum error, and the weight of each instance is updated. Each instance is finally classified using a function depending on the weighted average of the outputs from the weak classifiers, with weights defined as the boosting parameters and greater weights given to classifiers with lower errors. Different approaches have been used to determine the error of the weak learner, the boosting parameter, the weight update scheme, and the final decision rule, leading to a number of variants, such as gradient boosting [11], Real AdaBoost [12], LogitBoost [12], and Gentle AdaBoost [12].

Even though the AdaBoost method is a powerful tool for classification and learning, it has been employed only in a limited number of computer vision applications: classification of handwritten data [3], real time face detection [35], object tracking [26], classification of trees and vehicles in urban scenes [36], categorization of natural scenes [24], and keypoint detection and landmarking on human faces [8].

In particular, it has not yet been adapted for the evaluation and estimation of the reliabilities/weights of point matches established between overlapping 3D partial shapes determined by an FEM method, perhaps for several reasons. Firstly, registration ultimately represents a regression problem, rather than a classification problem. In some sense, all the point matches belong to

the same class but differ in how good a fit they are to the underlying transformation. Secondly, labelled training data is not available (AdaBoost is a supervised learning method). Thirdly, it may be challenging to identify suitable weak learners and formalize the problem using an additive model, making it difficult to adapt AdaBoost to this new task.

3 THE ITERATIVE RE-WEIGHTING METHOD

We now explain our novel algorithm. Given two overlapping 3D partial shapes, any representative FEM method, e.g. the SHOT algorithm [32] or the USC algorithm [32], can be employed to establish a set of PPMs $(\mathbf{p}_i, \mathbf{p}'_i)$ $(i = 1, 2, \cdots, N \geq 3)$ where the $\mathbf{p}_i$ come from the first shape and the $\mathbf{p}'_i$ from the second. Such point matches are typically contaminated by outliers. In this paper, we use a weight w_i in the interval $[0, 1]$ to represent the extent to which we believe match $(\mathbf{p}_i, \mathbf{p}'_i)$ to be correct, with a value of 1 meaning certainty. Our novel RIRW method iteratively estimates and updates these weights. Using the final weights allows more accurate weighted least-squares estimation of the underlying transformation. The iteration counter k is initialised to $k = 0$. All weights are initialized to $w_i^{(0)} = 1$; the superscript denotes the iteration. Our method is based on three ideas: underlying transformation estimation, penalty parameter estimation, and weight re-estimation and update, as described in the next subsection. We then summarise our algorithm, and finally compare the properties of our novel algorithm with AdaBoost and an M-estimator.

3.1 Derivation of main computational steps

Given the point matches $(\mathbf{p}_i, \mathbf{p}'_i)$, and their weights $w_i^{(k)}$, these weights are first normalised to sum to one. The underlying transformation parameters in the form of a rotation matrix $\mathbf{R}$ and translation vector $\mathbf{t}$ can be estimated in the weighted least squares sense using the following objective function:

$$J(\mathbf{R}, \mathbf{t}) = \sum_{i=1}^{N} w_i^{(k)} ||\mathbf{p}'_i - \mathbf{R}\mathbf{p}_i - \mathbf{t}||^2. \quad (1)$$

We use the quaternion method [5] to minimize this objective function, yielding an estimate of the rotation matrix $\mathbf{R}^{(k)}$ and translation vector $\mathbf{t}^{(k)}$. In order to reliably estimate $(\mathbf{R}, \mathbf{t})$, it is crucial to accurately estimate the weights $w_i^{(k)}$, which characterize the extent to which each point match $(\mathbf{p}_i, \mathbf{p}'_i)$ is correct. To this end, we build a new objective function based on the entropy maximization (EntMax) principle [13]:

$$\begin{aligned} J(\mathbf{W}^{(k+1)}) &= \sum_i w_i^{(k+1)} e_i^{(k)} \\ &+ \sum_i \frac{1}{\beta_i^{(k+1)}} w_i^{(k+1)} (\log w_i^{(k+1)} - 1) \quad (2) \end{aligned}$$

where $\mathbf{W}^{(k+1)} = \{w_1^{(k+1)}, w_2^{(k+1)}, \cdots, w_N^{(k+1)}\}$ and $e_i^{(k)} = ||\mathbf{p}'_i - \mathbf{R}^{(k)}\mathbf{p}_i - \mathbf{t}^{(k)}||$. This objective function minimizes the weighted average registration error $e_i^{(k)}$ of all PPMs $(\mathbf{p}_i, \mathbf{p}'_i)$, and maximizes the entropy of these weights $w_i^{(k+1)}$. In contrast with [13], which implicitly assumes that all point matches are of comparable quality and thus uses a single parameter β to balance the contribution of the two terms, we use individual parameters β_i to distinguish their varying correctnesses. Setting the first order derivative of this objective function with respect to $w_i^{(k+1)}$ to zero leads to:

$$w_i^{(k+1)} = \exp(-\beta_i^{(k+1)} e_i^{(k)}).$$

The key issue is thus to estimate the parameters $\beta_i^{(k+1)}$. To this end, we build another objective function again in the framework of entropy maximization:

$$\begin{aligned} J(\beta^{(k+1)}) &= \sum_i 2{\beta_i^{(k+1)}}^2 (e_i^{(k)} - e_\mu^{(k)})^2 - \\ & 2{e_\sigma^{(k)}}^2 \sum_i (2{\beta_i^{(k+1)}}^2 + 1) \left[\log(2{\beta_i^{(k+1)}}^2 + 1) - 1\right] \quad (3) \end{aligned}$$

where $\beta^{(k+1)} = \{\beta_1^{(k+1)}, \beta_2^{(k+1)}, \cdots, \beta_N^{(k+1)}\}$,

$$e_\mu^{(k)} = \sum_{i=1}^{N} w_i^{(k)} e_i^{(k)}$$

and

$$e_\sigma^{(k)} = \sqrt{\sum_{i=1}^{N} w_i^{(k)} (e_i^{(k)} - e_\mu^{(k)})^2}.$$

This objective function minimizes the weighted variance from $e_\mu^{(k)}$ of the registration errors $e_i^{(k)}$ for all PPMs $(\mathbf{p}_i, \mathbf{p}'_i)$; the weights $2{\beta_i^{(k+1)}}^2$ are regularized by their shifted entropy

$$B = \sum_i ((2{\beta_i^{(k+1)}}^2 + 1) \left[\log(2{\beta_i^{(k+1)}}^2 + 1) - 1\right].$$

The two terms are balanced by $2{e_\sigma^{(k)}}^2$. Then, setting the derivative with respect to $\beta_i^{(k+1)}$ of this objective function to zero gives

$$\beta_i^{(k+1)} = \sqrt{0.5(1 - \alpha_i^{(k)})/\alpha_i^{(k)}}$$

where

$$\alpha_i^{(k)} = \exp(-(e_i^{(k)} - e_\mu^{(k)})^2 / (2{e_\sigma^{(k)}}^2)).$$

In order to learn from previous iterations, we also take into account the current normalized weight $w_i^{(k)}$, so the weight in the new iteration is finally updated to be:

$$w_i^{(k+1)} = \max(w_i^{(k)}, w_i^{(k+1)}). \quad (4)$$

Firstly, this ensures that w_i remains in the interval $[0, 1]$. Secondly, taking the maximum of these weights better characterizes than other alternative schemes (like geometric mean) the extent to which a point match is correct,

no matter how accurately the rotation matrix $\mathbf{R}$ and translation vector $\mathbf{t}$ were estimated from past iterations. This observation is verified by the experimental results given in Section 4.2. Thirdly, the method can learn from both its good and poor estimates in successive iterations.

In sharp contrast to the main idea of the traditional AdaBoost algorithm, which boosts the weights of the misclassified instances and decreases the weights of the correctly classified instances, our algorithm penalizes all the matches $(\mathbf{p}_i, \mathbf{p}'_i)$ in a uniform manner according to their errors $e_i^{(k)}$ as well as their corresponding penalty parameters $\beta_i^{(k+1)}$. The larger the registration error and the penalty parameter of a point match, the more heavily this point match will be penalized, and the less likely this point match will be judged correct. Note that we do not classify the point matches as inliers or outliers, so there are no weak classifiers to adjust during iteration. We focus instead on the estimation of the weights of point matches, showing the extent to which they are believed to be reliable.

3.2 The iterative re-weighting algorithm

Pulling the previous ingredients together gives our proposed RIRW algorithm:

1: Use features to establish a set of point matches between two overlapping 3D partial shapes
2: Calculate the average distance s between the closest neighboring points in the original partial shapes, initialize the weight of each point match to 1, the maximum number $k_{\max}$ of iterations, iteration counter $k = 0$ and $e_\mu^{(0)} = \infty$
3: **while** $e_\mu^{(k)} > s$ and $k < k_{\max}$ **do**
4: Normalise the weights: $w_i^{k)} \leftarrow w_i^{(k)} / \sum_{j=1}^{N} w_j^{(k)}$
5: Estimate the solution $(\mathbf{R}^{(k)}, \mathbf{t}^{(k)})$ from Equation 1
6: Calculate the weighted average $e_\mu^{(k)}$ and standard deviation $e_\sigma^{(k)}$ of the point match errors
7: Estimate the penalty parameter $\beta_i^{(k+1)}$ for each point match using Equation 3
8: Estimate the weight $w_i^{(k+1)}$ of each point match using Equation 2
9: Update the weight $w_i^{(k+1)}$ of each point match using Equation 4
10: $k \leftarrow k + 1$
11: **end while**
12: Re-estimate the underlying transformation $(\mathbf{R}, \mathbf{t})$ from all point matches $(\mathbf{p}_i, \mathbf{p}'_i)$ using Equation 1

As each step has a computational complexity of $O(N)$ in the number N of established point matches between the overlapping partial shapes, the overall algorithm thus has a linear computational complexity $O(k_{\max}N)$. All experiments described later set $k_{\max} = 200$.

3.3 Analysis of the proposed method

Our proposed method has similarities to the AdaBoost and iteratively re-weighted least squares (IRLS) (M-estimator) methods. In this section, we compare and identify the differences that may lead to improved performance in evaluating the PPMs.

The boosting parameter β_i in Real AdaBoost in [12] is set to $\beta_i^{(k)} = 0.5 \log(\alpha_i^{(k)}/(1 - \alpha_i^{(k)}))$, and the new weight $w_i^{(k+1)}$ is set to $w_i^{(k+1)} = \exp(-\beta_i^{(k)} y_i)$, where an instance is classified into two classes with labels $y_i = \pm 1$. Clearly, if $\alpha_i^{(k)} > 0.5$ and this example is likely to be correctly classified with label $y_i = 1$, then $\beta_i^{(k)} > 0$ and $w_i^{(k+1)}$ will be decreased. However, if this example is incorrectly classified with label $y_i = -1$, then $w_i^{(k+1)}$ will be increased. If $\alpha_i^{(k)} < 0.5$ and this example is likely to be incorrectly classified with label $y_i = 1$, then $\beta_i^{(k)} < 0$, giving it a larger weight $w_i^{(k+1)}$, but if, this example is likely to be correctly classified with $y_i = -1$, then $w_i^{(k+1)}$ will be decreased. In either case, this scheme attempts to boost the incorrectly classified data, i.e. increases its weight. The boosting parameter β_i guarantees to optimize the objective function $E[\exp(-y_i F_i)]$ where $F_i = \text{sign}(\sum_{j=0}^{k} \beta_i^{(j)})$ is an additive model of the final classifier.

In contrast, our point match evaluation problem is quite different, lacking labelling information. It is essentially a continuous data fitting problem for the underlying transformation relating correct point matches. Our weight estimation scheme considers not just the penalty parameter $\beta_i^{(k+1)}$ but also the fitting error $e_i^{(k)}$. Both parameters vary significantly from one point match to another. The penalty parameter $\beta_i^{(k+1)}$ as defined in this paper is always positive: $\beta_i^{(k+1)} > 0$ and attempts to penalise those point matches whose errors are either much smaller or larger than $e_\mu^{(k)}$. Note that point matches with small errors are also penalised. To compensate for this penalty, the fitting error is taken into account. When $\alpha_i^{(k)} > 0.5$ and the point matches are likely to be correct, $\beta_i^{(k+1)} < \sqrt{0.5}$, leading to an increase in the associated weight. When $\alpha_i^{(k)} < 0.5$, the point matches are unlikely to be correct, unless they have small fitting errors: $\beta_i^{(k+1)} > \sqrt{0.5}$, leading to a decrease in weight. When $\alpha_i^{(k)} = 0.5$, then $e_i^{(k)} = e_\mu^{(k)} \pm \sqrt{2 \ln 2} e_\sigma^{(k)}$. This shows that the scheme actually increases weights of the point matches with either small fitting errors or fitting errors $e_i^{(k)}$ in the range of $[e_\mu^{(k)} - 1.177 e_\sigma^{(k)}, e_\mu^{(k)} + 1.177 e_\sigma^{(k)}]$, but reduces the weights of the point matches with large fitting errors. While the fitting error $e_i^{(k)}$ measures the error of a particular match and thus evaluates point matches separately, giving a bias against point matches with small errors, the penalty parameter $\beta_i^{(k+1)}$ considers the spread of errors over all the point matches and thus evaluates them as a whole, providing a more complete picture of correctness. A combination of these two factors better characterizes the extent $w_i^{(k+1)}$ to which a point match is correct.

AdaBoost and our RIRW method differ in five ways. Firstly, the former requires labeled data for training various weak and strong learners; labeled data is neither

available nor required in our method. Secondly, the boosting parameter in the former may be positive, zero, or negative, while it is always positive in our method. Thirdly, while the former attempts to boost incorrectly classified examples through learning from both their labels and penalty parameters, the latter attempts to penalize those point matches whose fitting errors are much larger than the weighted average point matching error. Fourthly, the boosting parameter in the former optimizes the objective function $E[\exp(-y_i F_i)]$, while the latter minimizes the weighted variance of the registration errors of the point matches. Fifthly, while the former eventually classifies each instance into one of two classes, the latter estimates the extent to which each point match is correct, for the purpose of optimizing the underlying transformation in a weighted least squares sense.

Our proposed algorithm is also in the spirit of IRLS (M-estimator) [2], [16], [38]. One of the best IRLS methods uses Tukey's biweight function [2]:

$$w(x) = \begin{cases} (1-(x/c)^2)^2 & \text{if } |x| \le c, \\ 0 & \text{otherwise.} \end{cases}$$

where x is the normalized fitting error of any point match $(\mathbf{p}_i, \mathbf{p}'_i)$: $x = (e_i^{(k)} - e_\mu^{(k)})/\delta$, $\delta = 1.48621(1+5/(N-6))\text{median}(e_i^{(k)})$, and $c = 4.6851 \times 0.0625$. Using Tukey's biweight function and our proposed method differ in two ways: Firstly, the former uses heuristics to classify point matches into two classes with different weights, while the latter treats all point matches uniformly, penalizing them according to their fitting errors and penalty parameters. Secondly, the former needs a data dependent threshold c, but our method is parameter free.

4 Experimental results

In this section, we use real data to demonstrate the proposed RIRW algorithm for evaluating N point matches $(\mathbf{p}_i, \mathbf{p}'_i)$ established using the SHOT features [32] unless otherwise stated, or USC features [33]. A comparative study was performed using methods from each of the three categories discussed in Section 2: from structural consistency based methods, we used common visual pattern discovery (CVPD) [18], from transformation consistency based methods we used RANSAC [32] and sparse vector field consensus (SparseVFC) [22], and from statistical regression methods, we used IRLS (M-estimator) based on Tukey's biweight function [38].

The aim of this study was to understand which method can most effectively evaluate the established point matches in the sense of producing the most accurate estimation of the underlying transformation relative to a refined estimate produced by ICP. In detail, the estimated underlying transformation was used to initialize an ICP variant, SoftICP [17] which usually produces accurate results after refinement. These results can be used to assess the performance of different methods under test [34]; this approach is particularly useful when ground truth concerning either the point matches or the underlying transformation is partially or completely unavailable, as is the case for the data used in this paper.

All real data in Figure 1 were downloaded from [25]; they were captured using a Minolta Vivid 700 range camera with a fixed resolution of 200×200 or a Technical Arts 100X range scanner with resolution varying from 86×129 to 240×240. The percentage relative errors $e_{\mathbf{h}}$, e_θ, and $e_{\mathbf{t}}$ in the rotation axis $\mathbf{h}$, rotation angle θ, and translation vector $\mathbf{t}$ of the finally estimated underlying transformation were computed. Further quantitative measures of the performance of the methods are the time taken for point match evaluation, and estimation of the underlying transformation refined by the SoftICP algorithm.

To illustrate the extent to which the established point matches are corrupted by false mathches and how challenging they are to evaluate, we also calculated the proportion e_c of correct point matches as a percentage: $e_c = n/N \times 100\%$ where n is the number of the correct matches. A correct match is taken to be a point match whose error e_i is smaller than 4 times the average distance between the closest neighboring points in the original shapes, measured using the underlying transformation estimated from the point matches evaluated by our RIRW method and refined by the SoftICP algorithm.

Our experimental study concerned four issues: registration error definition, the weight accumulation scheme within our RIRW algorithm, and studies comparing the RIRW algorithm and competing ones using two different databases. Experimental results are presented in Figures 2–9 and Tables 1–4. For each pair of overlapping 3D partial shapes, we call the first the *data shape*, and the second the *reference shape*. In Figures 3, 5, 7 and 9, yellow represents the transformed data shape with the transformation estimated from the evaluated point matches, and green represents the reference shape. All experiments were carried out on a PC with an Intel Xeon E5620 processor with unoptimized C code written in Microsoft Visual Studio 2008.

4.1 Registration error definition

In our RIRW method, the registration error is defined as: $e_i = ||\mathbf{p}'_i - \mathbf{R}\mathbf{p}_i - \mathbf{t}||$, the Euclidean distance (ED) between the matched points $(\mathbf{p}_i, \mathbf{p}'_i)$. In this section, we experimentally investigate whether the squared Euclidean distance (SED) might produce better results than ED. To this end, the overlapping shapes valve20–10, valve10–0, pat108–144, pat144–180, lobster0–20, lobster20–40, pooh140–160, and pooh160–180 in Figure 1 were selected for the experiments; the results are presented in Figures 2 and 3 and Table 1.

They show that ED outperforms SED as a definition of registration error of point matches, leading to significantly lower mean and standard deviations of error in the estimated rotation axes, rotation angles, and translation vectors of the underlying transformations. For example, SED results in significant displacement of

TABLE 1
Average μ and standard deviation σ of relative errors $e_{\mathbf{h}}(\%)$, $e_\theta(\%)$, and $e_{\mathbf{t}}(\%)$ in the estimated rotation axis $\hat{\mathbf{h}}$, rotation angle $\hat{\theta}$, and translation vector $\hat{\mathbf{t}}$ and evaluation time ti in seconds using different definitions for e_i in our RIRW method.

Parameter	Metric	$e_{\mathbf{h}}$ (%)	e_θ (%)	$e_{\mathbf{t}}$ (%)	ti (sec)
μ	ED	3.61	-0.05	3.63	71.13
	SED	16.34	3.67	12.36	71.75
σ	ED	4.17	3.12	3.53	21.15
	SED	32.28	15.39	18.56	22.27

TABLE 2
Average μ and standard deviation σ of relative errors $e_{\mathbf{h}}(\%)$, $e_\theta(\%)$, and $e_{\mathbf{t}}(\%)$ of the estimated rotation axis $\hat{\mathbf{h}}$, rotation angle $\hat{\theta}$, and translation vector $\hat{\mathbf{t}}$ and evaluation time ti in seconds using different schemes for combining weights from different iterations in our RIRW method.

Param.	Scheme	$e_{\mathbf{h}}$ (%)	e_θ (%)	$e_{\mathbf{t}}$ (%)	ti (sec)
μ	MAX	4.35	-0.26	5.87	38.88
	GEM	6.94	-1.30	8.76	39.00
	MIN	6.89	-4.69	9.35	39.62
σ	MAX	3.66	5.84	5.46	25.38
	GEM	6.62	6.76	8.93	23.93
	MIN	8.59	11.22	8.27	24.50

the transformed pat108 data shape relative to the pat144 reference shape.

Since the established point matches are heavily corrupted by outliers, SED strongly penalizes matches with larger errors, tending to reject correct matches as outliers, and so sometimes loses balance in characterizing errors and reliable matches, failing to distinguish them. In extreme cases SED may even lead to underflow in the computations performed. Overall, ED provides a better compromise between penalising point matches with registration errors and accurate estimates of their reliabilities. Our results provides further evidence for the claims in [6] for feature matching and in [14] for noise removal that the L_2 norm, SED, is over-aggressive in rejecting data as outliers compared to the L_1 norm, ED. This justifies our use of the L_1 norm, ED.

4.2 Weight accumulation

The RIRW algorithm combines the weights estimated in successive iterations. Various schemes can be used for this task. We investigated three different schemes: $w_i^{(k+1)} = \max(w_i^{(k)}, w_i^{(k+1)})$, $w_i^{(k+1)} = \sqrt{w_i^{(k)} w_i^{(k+1)}}$, and $w_i^{(k+1)} = \min(w_i^{(k)}, w_i^{(k+1)})$, which we denote maximum (MAX), geometric mean (GEM), and minimum (MIN) in the rest of this section. We note that $\max(w_i^{(k)}, w_i^{(k+1)}) \geq \sqrt{w_i^{(k)} w_i^{(k+1)}} \geq \min(w_i^{(k)}, w_i^{(k+1)})$. The overlapping bluedino125–375, reddino0–36, bird20–40, buddha40–60, lobster60–80, lobster80–100, cow50-47, and cow47–44 shapes in Figure 1 were selected for these experiments; the results are presented in Figures 4 and 5 and Table 2.

No single scheme always produces the most accurate results. However, the MAX scheme is the most stable and produced the most accurate evaluation results overall. Both the GEM and MIN schemes lead to failures: the transformed data cow50 shape intersected the reference cow47 shape, rather than overlapping it correctly. The MAX scheme has on average lowest relative errors in the estimated rotation axis, rotation angle and translation vector over the eight pairs of the overlapping shapes. The GEM scheme is affected by the penalty parameters and underlying transformations inaccurately estimated in certain iterations, while the weights selected by the MIN scheme from different iterations are not always representative of the actual quality of the point matches. The weights from the MAX scheme are more informative in distinguishing between correct and false matches, benefiting from an accurate estimate of the weights of the point matches in any iteration. These results justify our selection of the MAX scheme.

4.3 SHOT feature matches, Minolta Vivid 700 data

This section provides a comparative study of different techniques: RANSAC [9], Tukey's biweight function based IRLS [38], CVPD [18], SparseVFC [22] and our RIRW method using matches based on SHOT features [32]. The overlapping tubby0–20, tubby20–40, frog0–40, frog40–80, duck0–20, bird0–20, bunny0–40 and cow37–40 shapes in Figure 1 were used in these experiments; the results are presented in Figures 6 and 7 and Table 3. The percentages e_c of correct point matches among the ones established between these shapes are 21.83%, 22.36%, 3.32%, 4.38%, 6.82%, 11.76%, 4.07%, and 31.67% respectively; note that these are always less than 50%, and much less in some cases.

The results show that the CVPD method failed to correctly identify the common patterns defined by the point matches between the frog0-40 and bunny0-40 shapes. The RANSAC and CVPD methods failed to successfully downweight bad point matches between the frog40-80 shapes. The SparseVFC methods failed to accurately estimate the weights of the point matches between the frog0-40 and frog40-80 shapes. The RANSAC, IRLS, CVPD and SparseVFC methods also determined unsuitable weights for the point matches between the duck0-20, bird0-20 and cow37-40 shapes. However, our RIRW method determined suitable weights for the point matches for all 8 pairs of overlapping shapes. Failures are manifested by the fact that the transformed frog0, bunny0, and frog40 data shapes intersect the frog40, bunny40 and frog80 reference shapes in 3D space. Inaccurate evaluation of point matches leads the transformed duck0, bird0, and cow37 shapes to be displaced around the beaks of the duck and the bird, and the head of the cow, compared to the reference duck20, bird20, and cow40 shapes.

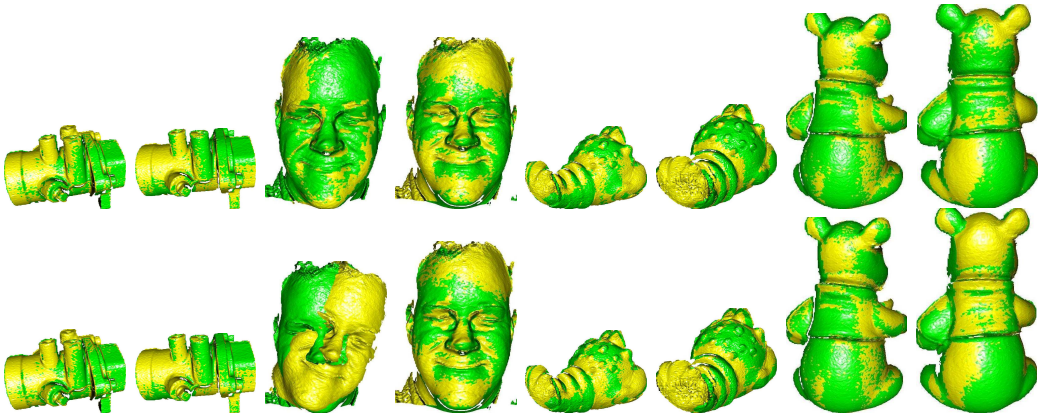

Fig. 2. Final registration results of different overlapping partial shapes for our RIRW method, using different definitions of e_i: top row: ED; bottom row: SED. Left to right: valve20–10, valve10–0, pat108–144, pat144–180, lobster0–20, lobster20–40, pooh140–160, and pooh160–180.

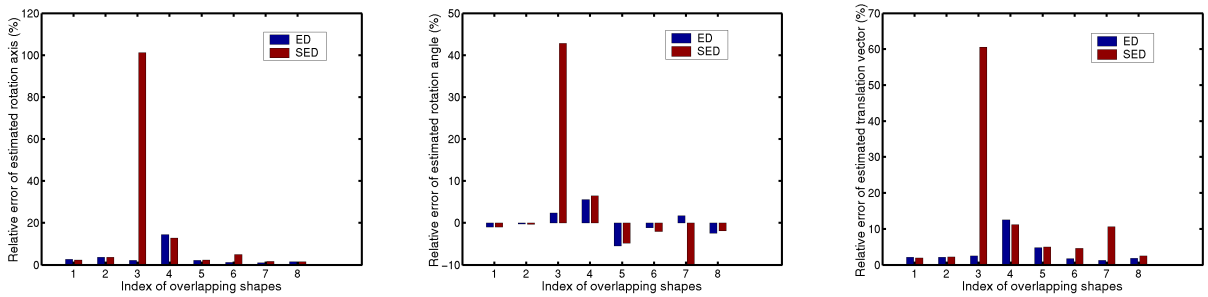

Fig. 3. The average μ and standard deviation σ of the relative errors $e_{\mathbf{h}}(\%)$, $e_{\theta}(\%)$, and $e_{\mathbf{t}}(\%)$ of the estimated rotation axis $\hat{\mathbf{h}}$ (left), rotation angle $\hat{\theta}$ (middle), and translation vector $\hat{\mathbf{t}}$ (right) for our RIRW method with parameter e_i taking different definitions. Indexes 1 through 8 represent the overlapping shape pairs valve20–10, valve10–0, pat108–144, pat144–180, lobster0–20, lobster20–40, pooh140–160, and pooh160–180 respectively.

These observations are verified in Figure 7 and Table 3, showing that the proposed RIRW method provided the most accurate and stable estimates of the underlying transformation from the weighted point matches established by the SHOT method. In the RANSAC method, difficult choices must be made [29] for the threshold used to distinguish inliers from outliers, and to specify the goodness of a model, while the IRLS method has difficulties in classifying the PPMs into two categories with different weights. The CVPD method must estimate the adjacency matrix for the description of visual patterns and has difficulties in identifying common visual patterns in different overlapping shapes, while the SparseVFC method imposes few constraints and has $3N$ degrees of freedom, which is much larger than the 6 needed to model the underlying rigid transformation, causing overfitting. In sharp contrast, the minimization of the weighted variance and average of the registration errors of the PPMs in our RIRW method provides a powerful and effective way of estimating the intermediate parameters of interest and thus their reliabilities.

Our proposed method is also fastest. The RANSAC method has to sample data and estimate the underlying transformation in each of many iterations, and it is difficult to decide when to terminate. The IRLS method has to sort the fitting errors of the PPMs, the CVPD method has to do many matrix and vector multiplications, and the SparseVFC method has to solve a linear system with many unknowns in each iteration. Our method computes simple statistics on the fitting errors of the point matches, and updates their weights using simple exponential and maximum operations. A further benefit is that its better estimates of the underlying transformation enable the SoftICP algorithm used for refinement to converge very quickly.

4.4 USC feature matches, Technical Arts 100X data

A similar comparative study was performed using the same methods, but USC features [33] and data captured by a Technical Arts 100X scanner. This enables us to check the generality of the conclusions drawn in the last section. The overlapping adapter2–3, agpart2–3, column2–5, curvblock1–2, grn-blk1–2, wye2–3, jumble11–12 and block2–3 shapes in Figure 1 were selected for the experiments; the results are presented in Figures 8 and 9 and Table 4. The percentages e_c of

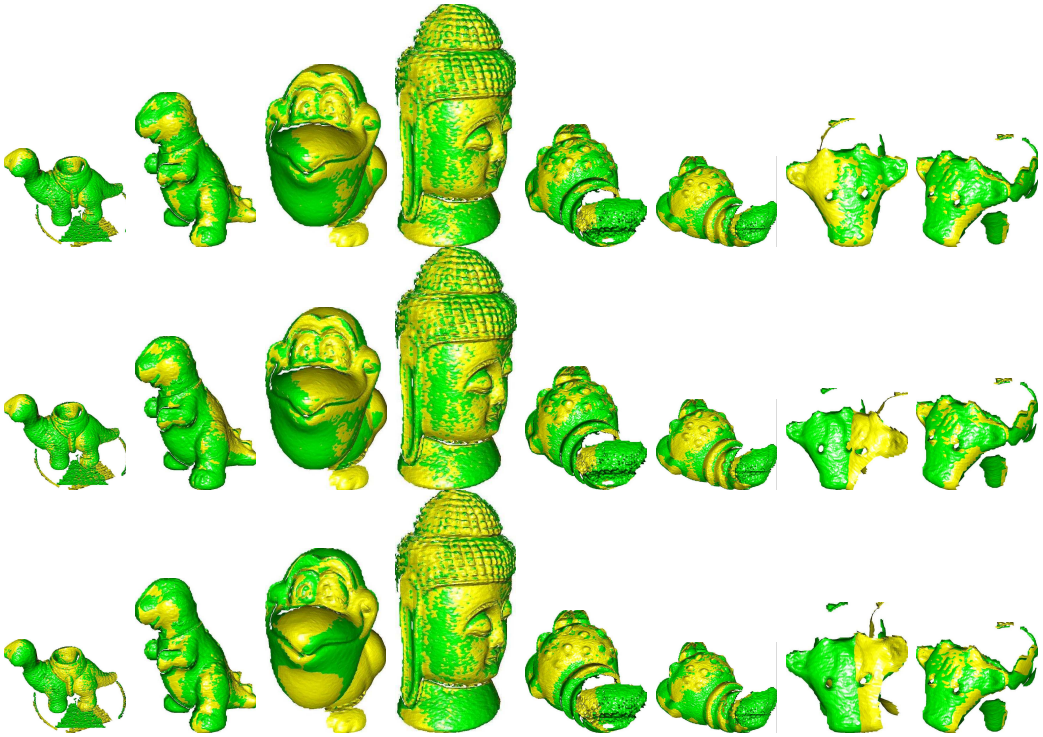

Fig. 4. Registration results of different overlapping partial shapes for our RIRW method, using different approaches for combining weights from different iterations. Left to right: bluedino125–375, reddino0–36, bird20–40, buddha40–60, lobster60–80, lobster80–100, cow50-47, and cow47–44. Top: MAX; Middle: GEM; Bottom: MIN.

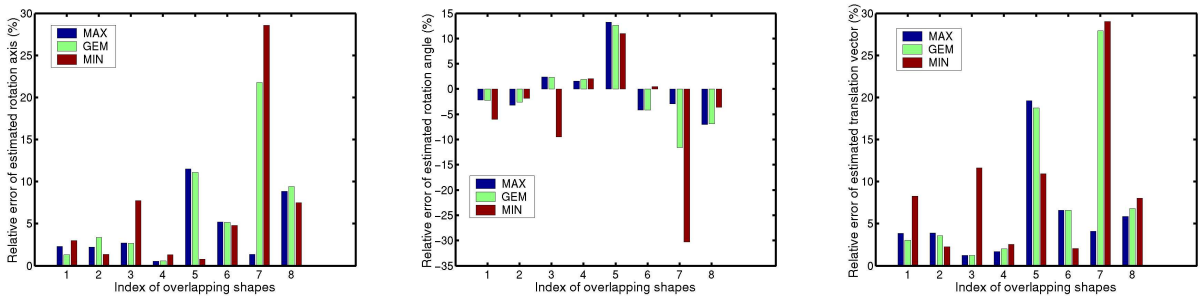

Fig. 5. Average μ and standard deviation σ of relative errors $e_{\mathbf{h}}(\%)$, $e_{\theta}(\%)$, and $e_{\mathbf{t}}(\%)$ of the estimated rotation axis $\hat{\mathbf{h}}$ (left), rotation angle $\hat{\theta}$ (middle), and translation vector $\hat{\mathbf{t}}$ (right) for our RIRW method, using different approaches for combining weights from different iterations. Indexes 1 through 8 represent bluedino125–375, reddino0–36, bird20–40, buddha40–60, lobster60–80, lobster80–100, cow50-47, and cow47–44 respectively.

correct point matches among the established ones were again low, being 23.32%, 11.43%, 9.27%, 2.94%, 11.20%, 1.18%, 2.49%, and 4.68% respectively.

The various methods show similar behavior to that observed in the last section. The IRLS, CVPD, and SparseVFC methods failed to successfully downweight the bad point matches between the column2–5 and block2–3 shapes, while the CVPD and SparseVFC methods failed to determine appropriate weights for point matches between the curvblock1–2 and wye2–3 shapes. As a result the transformed column2, block2, curvblock1, and wye2 data shapes intersect the column5, block3, curvblock2 and wye3 reference shapes in 3D space respectively. In sharp contrast, our RIRW method determined appropriate weights for the point matches between all the eight pairs of overlapping shapes, yielding an accurate estimation of the underlying transformation with good alignment. It is interesting to note that while the RANSAC and the proposed RIRW methods aligned the larger green blocks in the jumbles example, the IRLS, CVPD and SparseVFC methods made a compromise in aligning both the columns and the green blocks. See Figures 8 and 9.

The proposed RIRW method had lowest relative errors on average for the estimated rotation axis, rotation angle, and translation vector. Again, it was also the most

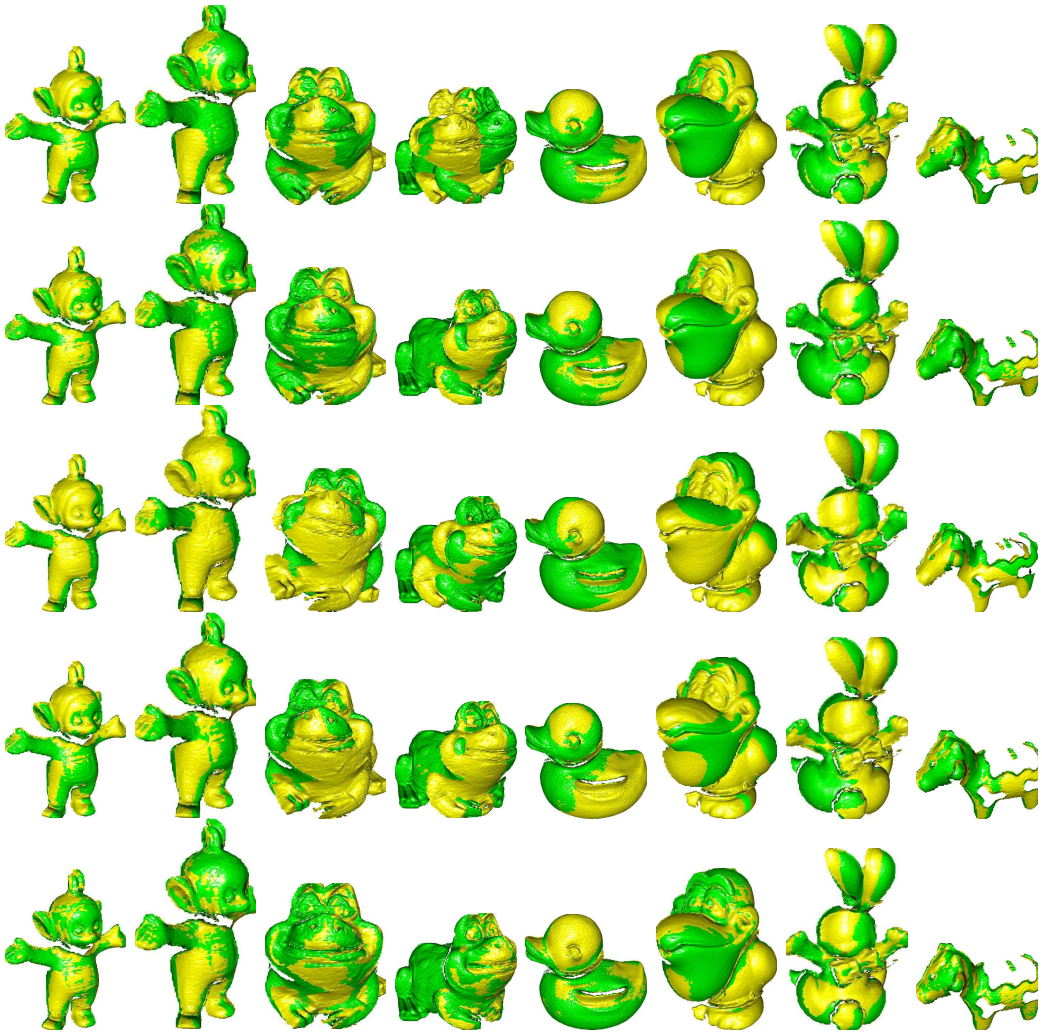

Fig. 6. Registration results of different overlapping partial shapes for different evaluation algorithms. Left to right: tubby0–20, tubby20–40, frog0–40, frog40–80, duck0–20, bird0–20, bunny0–40 and cow37–40. Top row: RANSAC; Second: IRLS; Third: CVPD; Fourth: SparseVFC; Bottom: RIRW.

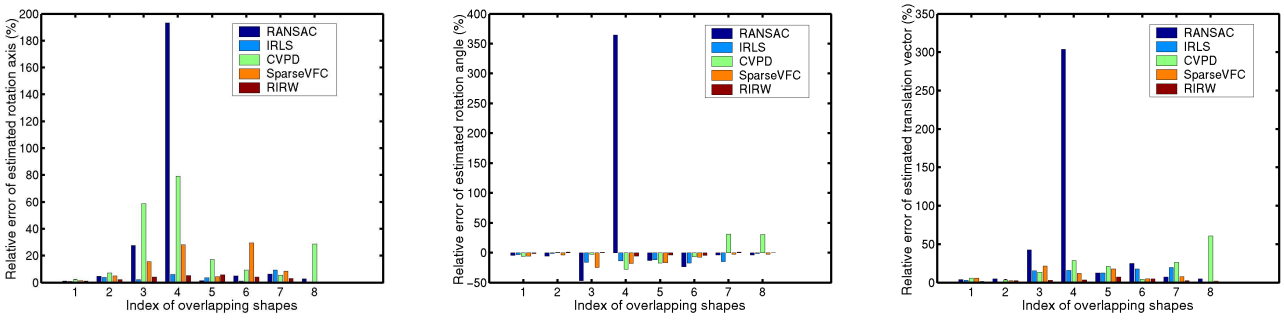

Fig. 7. Average μ and standard deviation σ of relative errors $e_{\mathbf{h}}(\%)$, $e_{\theta}(\%)$, and $e_{\mathbf{t}}(\%)$ of the estimated rotation axis $\hat{\mathbf{h}}$ (left), rotation angle $\hat{\theta}$ (middle), and translation vector $\hat{\mathbf{t}}$ (right) for different algorithms. Indexes 1 through 8 represent tubby0–20, tubby20–40, frog0–40, frog40–80, duck0–20, bird0–20, bunny0–40 and cow37–40 respectively.

computationally efficient method. These results show that the proposed RIRW method is powerful and can stably estimate the underlying transformation from point matches based on different features using data captured by various scanners.

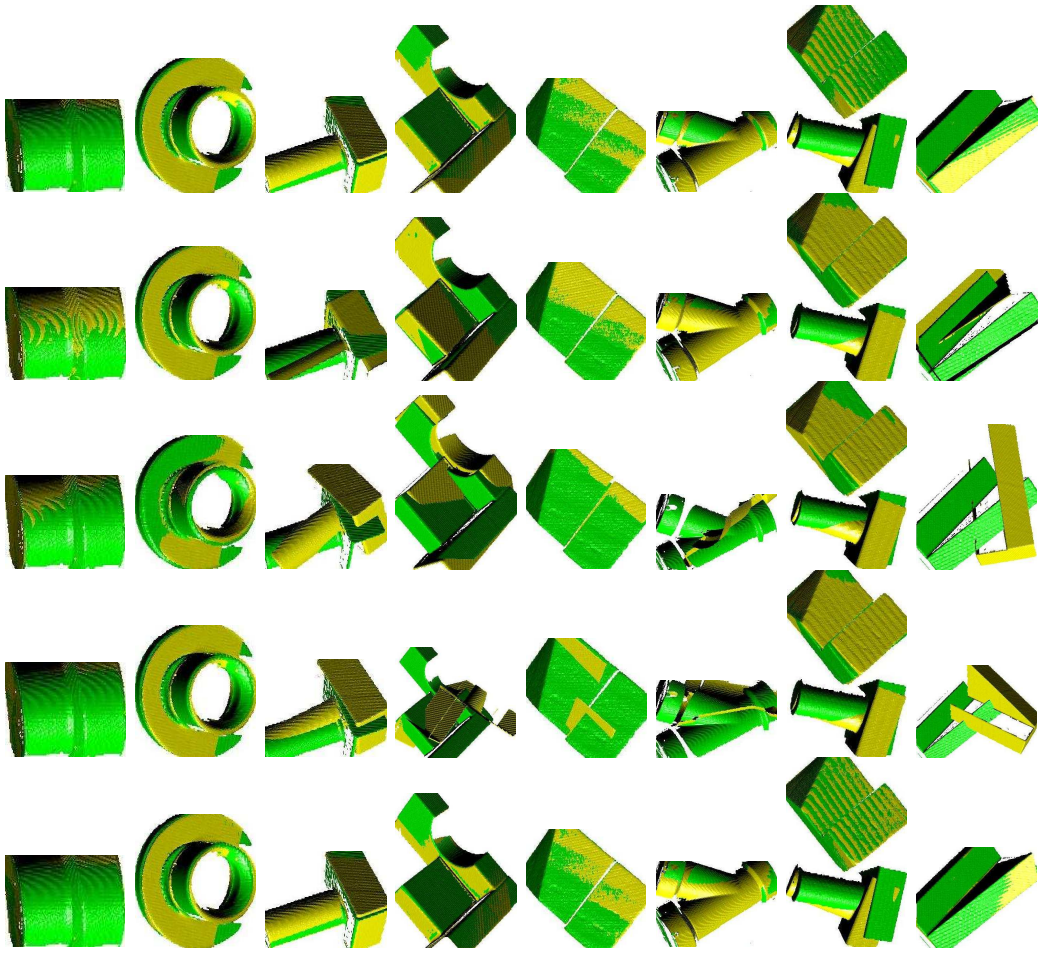

Fig. 8. Registration results of different overlapping partial shapes for different evaluation algorithms. Left to right: adapter2–3, agpart2–3, column2–5, curvblock1–2, grn-blk1–2, wye2–3, jumble11–12 and block2–3. Top row: RANSAC; Second: IRLS; Third: CVPD; Fourth: SparseVFC; Bottom: RIRW.

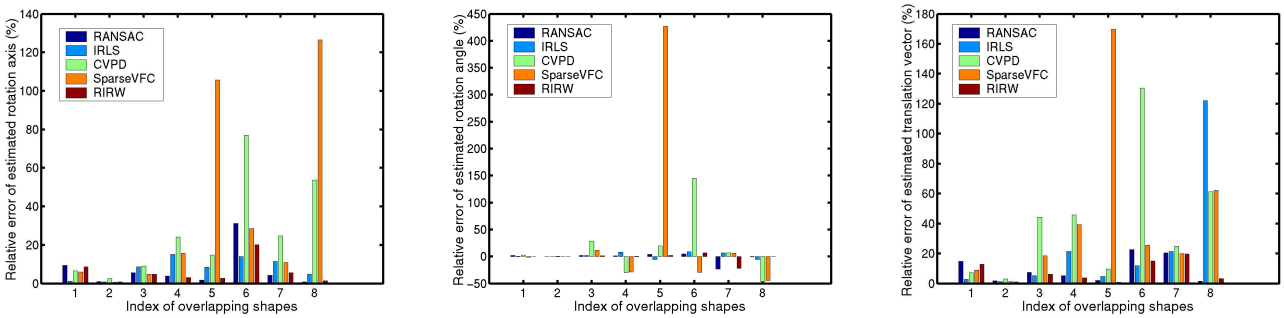

Fig. 9. Average μ and standard deviation σ of relative errors $e_{\mathbf{h}}(\%)$, $e_{\theta}(\%)$, and $e_{\mathbf{t}}(\%)$ of the estimated rotation axis $\hat{\mathbf{h}}$ (left), rotation angle $\hat{\theta}$ (middle), and translation vector $\hat{\mathbf{t}}$ (right) for different algorithms. Indexes 1 through 8 represent adapter2–3, agpart2–3, column2–5, curvblock1–2, grn-blk1–2, wye2–3, jumble11–12 and block2–3 respectively.

5 Conclusions

Feature extraction followed by matching is widely used for registering overlapping 3D partial shapes. Our experimental results show that unfortunately, up to 99% of the point matches established can be outliers with unpredictable errors, and they are thus extremely challenging to evaluate. Our new method is based on two main steps, using two objective functions to estimate penalty parameters first and then weights. After initializing or estimating weights of the PPMs, the underlying transformation is estimated in the weighted least squares sense, allowing computation of the weighted average e_{μ} and

TABLE 3
Average μ and standard deviation σ of the relative errors $e_{\mathbf{h}}(\%)$, $e_\theta(\%)$, and $e_{\mathbf{t}}(\%)$ of the estimated rotation axis $\hat{\mathbf{h}}$, rotation angle $\hat{\theta}$, and translation vector $\hat{\mathbf{t}}$ and evaluation time ti in seconds for different algorithms.

Para.	Algo.	$e_{\mathbf{h}}$ (%)	e_θ (%)	$e_{\mathbf{t}}$ (%)	ti (sec)
μ	RANSAC	30.38	33.16	50.74	73.75
	IRLS	3.51	-9.80	10.84	44.50
	CVPD	26.07	0.35	20.70	62.63
	SparseVFC	11.78	-10.15	9.52	44.50
	RIRW	3.35	-1.42	3.29	42.75
σ	RANSAC	62.16	126.15	96.53	74.26
	IRLS	2.90	6.40	7.31	36.84
	CVPD	26.47	19.50	17.79	64.78
	SparseVFC	10.84	-10.15	9.52	38.66
	RIRW	1.77	2.54	1.89	34.95

TABLE 4
Average μ and standard deviation σ of relative errors $e_{\mathbf{h}}(\%)$, $e_\theta(\%)$, and $e_{\mathbf{t}}(\%)$ of the estimated rotation axis $\hat{\mathbf{h}}$, rotation angle $\hat{\theta}$, and translation vector $\hat{\mathbf{t}}$ and evaluation time ti in seconds for different algorithms.

Para.	Algo.	$e_{\mathbf{h}}$ (%)	e_θ (%)	$e_{\mathbf{t}}$ (%)	ti (sec)
μ	RANSAC	7.31	-1.09	9.53	54.63
	IRLS	8.09	2.07	23.95	72.37
	CVPD	26.55	16.09	40.89	65.87
	SparseVFC	37.41	42.69	43.27	177.75
	RIRW	5.94	-1.20	7.93	54.00
σ	RANSAC	9.41	8.46	8.12	42.22
	IRLS	5.10	5.27	37.89	48.47
	CVPD	24.32	54.08	39.13	46.79
	SparseVFC	46.43	146.51	50.93	260.75
	RIRW	5.84	7.98	6.69	42.09

variance e_σ^2 of the registration errors over all PPMs. The first objective function aims to minimize the weighted variance from e_μ of the registration errors of the PPMs with the weights defined by the penalty parameters, regularized by their shifted entropy and balanced by $2e_\sigma^2$. The second aims to minimize the weighted average of the registration errors of the PPMs with the weights regularized by their entropy and balanced by their penalty parameters. The result is that the reliability of each point match is accurately characterized by a real number in the unit interval, leading to an accurate estimation of the underlying transformation via weighted least-squares.

Our contributions can be summarized as follows. Firstly, we have provided a novel regularization based iterative re-weighting method for evaluating point matches between two overlapping 3D partial shapes, assuming that matches have already been established by any chosen FEM method. Point matches are treated as having different reliabilities, and are accordingly weighted both when re-estimating these reliabilities, and when using the point matches to estimate the underlying transformation. Our method provides a generic and principled framework for the task based on a mathematically elegant approach. It is easily implemented, has a closed form solution, and does not depend on any arbitrary parameters.

Secondly, our comparative study based on real data captured by two different laser scanners shows that regularization based objective functions provide a powerful means for estimation of transformation parameters. The proposed method outperforms four selected state-of-the-art methods: RANSAC, IRLS, CVPD, and SparseVFC, providing accurate and stable estimation of the underlying transformation from point matches established by two different FEM methods. It significantly improves upon a coarse pose estimate provided by using all matches in an unweighted combination, an approach often used in practice to initialise fine registration using the ICP algorithm or some variant. Better initialization results in the latter being more likely to find a correct global minimum, providing more accurate and robust registration results; fewer ICP iterations are also required with better initialization.

Thirdly, our study shows that even though up to 99% of the established point matches may be outliers, use of our algorithm can still lead to accurate recovery of the underlying transformation with errors as small as 5% relative to the globally optimal solution. Indeed, for some applications, such errors may be low enough to avoid having to use refinement at all.

Finally, our results also show that the point matches established by typical FEM methods may not be as bad as they appear and may include more information than expected. More work is needed on the development of point match *evaluation* methods; novel *features* have attracted far more attention, but the former may provide greater opportunities for improving registration results.

While our RIRW method is computationally efficient and converges very quickly, more is needed to theoretically investigate its convergence properties: does it always converge within a limited number of iterations and have limited error after convergence, like AdaBoost? Incorporating a rigidity constraint is also likely to further improve the results provided by our method.

ACKNOWLEDGMENTS

We would like to express our sincere thanks to both the anonymous associate editor and reviewers for their constructive comments that have improved the quality and readability of the paper.

REFERENCES

[1] "AdaBoost", *http://en.wikipedia.org/wiki/AdaBoost*
[2] K.V. Arya, P. Gupta, P.K. Kala, P. Mitra, "Image registration using robust M-estimators", *Pattern Recognit. Letters*, vol. 28, pp. 1957-1968, 2007.
[3] T.R. Babu, M.N. Murty, V.K. Agrawal, "Adaptive boosting with leader based learners for classification of large handwritten data", *Proc. Four Int. Conf. Hybrid Intelligent Systems (HIS'04)*, 2004, pp. 326-331.
[4] J. Behley, V. Steinhage, A.B. Cremers, "Performance of histogram descriptors for the classification of 3D laser range data in urban environments", *Proc. ICRA*, 2012, pp. 4391-4398.
[5] P.J. Besl, N.D. McKay, "A method for registration of 3D shapes", *IEEE Trans. PAMI*, vol. 14, pp. 239-256, 1992.

[6] Z.-Q. Cheng, Y. Chen, R.R. Martin, Y.-K. Lai, A. Wang, "SuperMatching: feature matching using supersymmetric geometric constraints", *IEEE Trans. Visualization and Computer Graphics*, vol. 19, pp. 1885-1894, 2013.

[7] T. Cour, P. Srinivasan, J. Shi, "Balanced graph matching", *Proc. NIPS*, 2006, pp. 313-320.

[8] C. Creusot, N. Pears, J. Austin, "A machine learning approach to keypoint detection and landmarking on 3D meshes", *Int. J. Comput. Vis.*, vol. 102, pp. 146-179, 2013.

[9] M.A. Fishler, R.C. Bolles, "Random sample consensus: a paradigm for model fitting with applications to image analysis and automated cartography", *Comm. ACM*, vol. 24, no. 6, pp. 381-295, 1981.

[10] Y. Freund, R.E. Schapire, "A decision-theoretic generation of online learning and application to boosting", *Journal of Computer and System Science*, vol. 55, pp. 119-139, 1997.

[11] J.H. Friedman", Greedy function approximation: a gradient boosting machine", *Technical report, Department of Statistics, Standford University*, 1999.

[12] J.H. Friedman, T. Hastie, R. Tibshirani, "Additive logistic regression: a statistical view of boosting", *Ann. Statist.*, vol. 28, pp. 337-407, 2000.

[13] S. Gold, A. Rangarajan, C.-P. Lu, S. Pappu and E. Mjolsness, "New algorithms for 2-D and 3-D point matching: pose estimation and correspondence", *Pattern Recognit.*, vol. 31, pp. 1019-1031, 1998.

[14] T. Goldstein, S. Osher, "The split Bregman method for L1 regularized problems", *SIAM J. Imaging Sciences*, vol. 2, pp. 323-343, 2009.

[15] A. Johnson and M. Hebert, "Surface matching for object recognition in complex three-dimensional scenes", *Image and Vision Computing*, vol. 16, pp. 635-651, 1998.

[16] X.Li, Z. Hu,"Rejecting mismatches by correspondence function", *Int. J. Comput. Vis.*, vol. 89, pp. 1-17, 2010.

[17] Y. Liu, "Automatic 3d free form shape matching using the graduated assignment algorithm", *Pattern Recognit.*, vol. 38, pp. 1615-1631, 2005.

[18] H. Liu, S. Yan, "Common visual pattern discovery via spatially coherent correspondences", *Proc. CVPR*, 2010, pp. 1609-1616.

[19] T.R. Lo, and J.P. Siebert, "Local feature extraction and matching on range images: 2.5D SIFT", *Comput. Vis. Image Understand*, vol. 113, pp. 1235-1250, 2009.

[20] J. Ma, J. Zhao, J. Tian, A.L. Yuille, Z. Tu, "Robust point matching via vector field consensus", *IEEE Trans. Image Process.*, 23(2014) 1706-1721.

[21] J. Ma, J. Zhao, J. Tian, Z. Tu, A. Yuille, "Robust estimation of nonrigid transformation for point set registration", *Proc. CVPR*, 2003, pp. 2147-2154.

[22] J. Ma, J. Zhao, J. Tian, X. Bai, Z. Tu, "Regularizing vector field learning with sparse approximation for mismatch removal", *Pattern Recognit.*, vol. 46, pp. 3519-3532, 2013.

[23] J. Ma, J. Zhao, Y. Zhou, J. Tian, "Mismatch removal via coherent spatial mapping", *Proc. ICIP*, 2012, pp. 1-4.

[24] R. Nock, P. Piro, F. Nielsen, W.B.H. Ali, M. Barlaud, "Boosting k-NN for categorization of natural scenes", *Int. J. Comput. Vis.*, vol. 100, pp. 294-314, 2012.

[25] OSU(MSU/WSU) range image database. *http://sampl.ece.ohio-state.edu/data/3DDB/RID/index.htm.*

[26] T. Parag, F. Porikli, A. Elgammal, "Boosting adaptive linear weak classifiers for online learning and tracking", *Proc. CVPR*, 2008, pp. 1-8.

[27] K. Pathak, A. Birk, N. Vaskevicius, J. Popinga, lq'Fast registration based on noisy planes with unknown correspondences for 3-D mapping", *IEEE Trans. PAMI*, vol. 26, pp. 424-441, 2010.

[28] S. Ramalingam, Y. Taguchi, "A theory of minimal 3D point to 3D plane registration and its generalization", *Int. J. Comput. Vis.*, vol. 102, pp. 73-90, 2013.

[29] "RANSAC." http://en.wikipedia.org/wiki/RANSAC.

[30] S. Rusinkiewicz, M. Levoy, "Efficient variants of the ICP algorithm", *Proc. Int. Conf. 3D Digital Imaging and Modeling (3DIM)*, 2001, pp. 145-152.

[31] G.K.L. Tam, R.R. Martin, P.L. Rosin, Y.-K. Lai, "Diffusion pruning for rapidly and robustly selecting global correspondences using local isometry", *ACM Trans. Graphics*, vol. 33, Article 4, 2014.

[32] F. Tombari, S. Salti, L.D. Stefano, "Unique signatures of histograms for local surface description", *Proc. ECCV*, 2010, pp. 347-360.

[33] F. Tombari, S. Salti, L.D. Stefano, "Unique shape context for 3D data description", *Proc. 3DOR*, 2010, pp. 57-62.

[34] C. Torre-Ferrero, J.R. Llata, S. Robla, E.G. Sarabia, "A similarity measure for 3D rigid registration of point clouds using image-based descriptor with low overlap", *Proc. IEEE Int. Conf. Comput. Vis, Workshops*, 2009, pp. 71-78.

[35] P. Viola, M.J. Jones, "Robust real time face detection", *Int. J. Comput. Vis.*, vol. 57, pp. 137-154, 2004.

[36] Y. Wei, W. Yao, J. Wu, M. Schmitt, U. Stilla, "Adaboost-based feature relevance assessment in fusing LIDAR and image data for classification of trees and vehicles in urban scenes", *ISPRS Annals Photogrammetry, Remote Sensing Spatial Information Sciences*, vol. I-7, pp. 323-328, 2012.

[37] J. Yang, H. Li, Y. Jia, "Go-ICP: solving 3D registration efficiently and globally optimally", *Proc. ICCV*, 2013, pp. 1457-1464.

[38] Z. Zhang. "M-estimators", *http://research.microsoft.com/en-us/um/people/zhang/INRIA/Publis/Tutorial-Estim/node24.html*

[39] J. Zhao, J. Ma, J. Tian, J. Ma, D. Zhang, "A robust method for vector field learning with application to mismatch removing", *Proc. CVPR*, 2011, pp. 2977-2984

Yonghuai Liu is a senior lecturer at Aberystwyth University since 2011. His primary research interests lie in 3D computer vision, pattern recognition, image processing, and machine learning.

Luigi De Dominics is researcher from 1994 at ENEA, the Italian Agency for the New Technologies, Energy and the Economic Sustainable Development. From 2007 he is responsible for the development of laser scanner technologies for 3D underwater imaging. His areas of interest include 3D laser imaging, optical wireless communications and subsea positioning.

Baogang Wei is currently a professor at College of Computer Science and Technology of Zhejiang University. His main research interests include artificial intelligence, pattern recognition, and image processing.

Liang Chen is now a professor of Computer Science at University of Northern British Columbia, B.C, Canada. His research interests include pattern recognition, image processing, computational geometry, intelligent language tutoring system, data mining, and bioinformatics.

Ralph Martin obtained his PhD in 1983 from Cambridge University. Since then he has been at Cardiff University, as Professor since 2000, where he leads the Visual Computing research group. His publications include over 250 papers and 12 books covering such topics as solid modelling, computer graphics, and computer vision. He is a Fellow of the Learned Society of Wales, the Institute of Mathematics and its Applications, and the British Computer Society.